Exploring the Role of Macroalgal Surface Metabolites on the Settlement of the Benthic Dinoflagellate Ostreopsis cf. ovata

Eva Ternon, Benoît Paix, Olivier Thomas, Jean-François Briand, Gérald Culioli

frontiers in Marine Science

ORIGINAL RESEARCH
published: 21 August 2020
doi: 10.3389/fmars.2020.00683

Exploring the Role of Macroalgal Surface Metabolites on the Settlement of the Benthic Dinoflagellate *Ostreopsis* cf. *ovata*

Eva Ternon[1,2,3†], Benoît Paix[4†], Olivier P. Thomas[5], Jean-François Briand[4] and Gérald Culioli[4*]*

[1] CNRS, OCA, IRD, Université Côte d'Azur, Géoazur, Valbonne, France, [2] Laboratoire d'Océanographie de Villefranche, CNRS UMR 7093, Sorbonne Universités, Villefranche-sur-Mer, France, [3] Center for Marine Biotechnology and Biomedicine, Scripps Institution of Oceanography, University of California, San Diego, La Jolla, CA, United States, [4] Laboratoire MAPIEM, Université de Toulon, Toulon, France, [5] Marine Biodiscovery, School of Chemistry and Ryan Institute, National University of Ireland Galway, Galway, Ireland

OPEN ACCESS

Edited by:
Elisa Berdalet,
Institute of Marine Sciences (CSIC), Spain

Reviewed by:
Stefano Accoroni,
Marche Polytechnic University, Italy
Olga Carnicer,
Dalhousie University, Canada
Leo Lai Chan,
City University of Hong Kong, Hong Kong

***Correspondence:**
Eva Ternon
eva.ternon@imev-mer.fr
Gérald Culioli
culioli@univ-tln.fr

† These authors have contributed equally to this work

Specialty section:
This article was submitted to Marine Ecosystem Ecology, a section of the journal Frontiers in Marine Science

Received: 13 March 2020
Accepted: 28 July 2020
Published: 21 August 2020

Citation:
Ternon E, Paix B, Thomas OP, Briand J-F and Culioli G (2020) Exploring the Role of Macroalgal Surface Metabolites on the Settlement of the Benthic Dinoflagellate Ostreopsis cf. ovata. Front. Mar. Sci. 7:683. doi: 10.3389/fmars.2020.00683

Macroalgae constitute one of the preferred substrates of the benthic dinoflagellate *Ostreopsis* cf. *ovata*. Across the Mediterranean Sea, this toxic microalga has been shown to thrive on the surface of various species of macroalgae, including Chlorophyta, Rhodophyta, and Phaeophyceae. Interestingly, some Dictyotaceae are characterized by a low abundance of cells of *O.* cf. *ovata* on their surface. Based on the antifouling properties of some specialized metabolites produced by seaweeds, macroalgal metabolites have been proposed to contribute to the settlement and development of *O.* cf. *ovata*. To address this question, the composition of the surface of four Dictyotaceae, *Dictyota dichotoma*, *Dictyota spiralis*, *Taonia atomaria,* and *Padina pavonica* was investigated through an integrative approach combining the analysis of their eukaryotic diversity (18S rRNA gene metabarcoding), their surface metabolome (untargeted LC-MS-based metabolomics) as well as the bioactivity of their surface extracts on *O.* cf. *ovata*. Altogether, the data suggest an influence of the macroalgal surface chemistry on the growth of the dinoflagellate, with *D. dichotoma* being the most bioactive. Some metabolites are proposed to be involved in the observed bioactivity. Other biotic factors are also likely to be entailed in the control of the *O.* cf. *ovata* population and they may even prevail on the influence of the macroalgal surface chemistry.

Keywords: *Ostreopsis* cf. *ovata*, Dictyotaceae, surface colonization, metabolomics, metabarcoding, eukaryotes, biofilms

INTRODUCTION

Recurrent outbreaks of the toxic dinoflagellate *Ostreopsis* cf. *ovata* have been reported over the past 15 years in Mediterranean coastal waters (Ciminiello et al., 2006; Mangialajo et al., 2011). Despite recent research efforts (reviewed in Pistocchi et al., 2011; Carnicer et al., 2015), the abiotic factors fostering the proliferation of this species remain unclear (Cohu et al., 2011; Meroni et al., 2018) although high temperature, low hydrodynamic conditions seem to constitute a pre-requisite (Totti et al., 2010; Pezzolesi et al., 2012; Meroni et al., 2018). *O.* cf. *ovata* is a benthic species

that colonizes a variety of substrates, including macrophytes (Totti et al., 2010; Mangialajo et al., 2011). The surface of these seaweeds can constitute an ideal microenvironment for the growth of highly diverse prokaryotic and eukaryotic communities, including benthic microalgae. While the interactions between bacteria and macroalgae have been investigated to some extent during the past decades (Egan et al., 2013; Hollants et al., 2013), less information has been provided about the drivers guiding the settlement of microalgae on the surface of macroalgae.

Ostreopsis cf. *ovata* has been shown to thrive on the surface of various species of macroalgae across the Mediterranean Sea, including Chlorophyta (Battocchi et al., 2010; Accoroni et al., 2015; Hosny and Labib, 2019), Rhodophyta (Vila et al., 2001; Battocchi et al., 2010; Cohu et al., 2013; Blanfuné et al., 2015; Hosny and Labib, 2019; Gémin et al., 2020) and Phaeophyceae (Vila et al., 2001; Battocchi et al., 2010; Cohu et al., 2013; Blanfuné et al., 2015; Hosny and Labib, 2019; Gémin et al., 2020), without any clear species preference. Remarkably, some Phaeophyceae of the family Dictyotaceae are usually characterized by a low abundance of *O.* cf. *ovata* as for instance *Taonia atomaria*, *Dictyota fasciola,* or *Padina pavonica* (Blanfuné et al., 2015; Hosny and Labib, 2019; Gémin et al., 2020). The antifouling properties of some specialized metabolites produced by Dictyotaceae have been proposed to drive the settlement and development of *O.* cf. *ovata* (Cohu et al., 2013; Blanfuné et al., 2015; Gémin et al., 2020). Approaches in chemical ecology have revealed that metabolites produced by macroalgae can be detrimental or beneficial to the settlement of bacteria and microalgae (Goecke et al., 2010; Hellio et al., 2002; Wichard and Beemelmanns, 2018). In particular, several metabolites produced by species of the family Dictyotaceae have been shown to inhibit the growth of bacteria (e.g., dictyol C and fucoxanthin; Salvador Soler et al., 2007; Viano et al., 2009), microalgae (e.g., dictyolactone and sanadaol; Kim et al., 2006), bryozoan (e.g., dictyol E, pachydictyol A, dictyodial; Schmitt et al., 1998) and various other benthic species (e.g., diterpenoids, gleenol, and geranylgeranylglycerol; Bianco et al., 2009; Othmani et al., 2016b).

To the best of our knowledge, only one study has investigated the effect of the metabolites from brown, red and green macroalgae (*Dictyota dichotoma*, *Rhodymenia pseudopalmata,* and *Ulva rigida*, respectively) on the growth of the dinoflagellate *O.* cf. *ovata* (Accoroni et al., 2015). The exposure to dried algal cells, fresh thalli and dissolved metabolites of *D. dichotoma* caused an intense stress to *O.* cf. *ovata* cells yielding to growth inhibition as well as formation of double-walled cysts. Conversely, this inhibiting activity of *D. dichotoma* metabolites on the toxic dinoflagellate does not mirror the frequent development of *O.* cf. *ovata* on *D. dichotoma* observed in previous studies performed in the NW Mediterranean Sea (Cohu et al., 2013; Blanfuné et al., 2015; Gémin et al., 2020). Following common practices in the chemical ecology of macroalgae (Puglisi et al., 2014), the authors used whole-cell macroalgal extracts which are not representative of real ecological situations occurring at the surface of macroalgae. Therefore, the influence of the surface metabolome of brown algae on the growth and settlement of *O.* cf. *ovata* remains largely to be assessed. Results of such studies will provide valuable information on the pattern of colonization of this toxic dinoflagellate along the NW Mediterranean shoreline that leads to ecological (Gorbi et al., 2013; Giussani et al., 2016; Pavaux et al., 2019) and health (Ciminiello et al., 2006; Casabianca et al., 2013) concerns.

The epiphytic community colonizing the surface of macroalgae is not only expected to contribute to the surface metabolome but also to directly interact with *O.* cf. *ovata*, adding another level of complexity to its settlement preferences. Among co-occurring species on surfaces colonized by *O.* cf. *ovata*, *Roseobacter* bacteria (Vanucci et al., 2016; Guidi et al., 2018), diatoms of the genera *Licmophora*, *Navicula,* and *Amphora*, and the dinoflagellates *Prorocentrum lima*, *Amphidinium carterae*, and *Coolia monotis* (Accoroni et al., 2015; Marro et al., 2019) have been reported to be the most abundant. Recent evidences of chemically mediated interactions between microalgae and their predators (Ianora et al., 2004; Selander et al., 2015), competitors (Tillmann and Hansen, 2009; Poulson-Ellestad et al., 2014; Ternon et al., 2018), and the bacterial community (Wichard and Beemelmanns, 2018 and references therein) suggest that biotic interactions within members of the epiphytic community may also influence the settlement of *O.* cf. *ovata* on macroalgal surfaces.

This study aims to investigate the influence of the surface metabolome of four brown algae of the Dictyotaceae family (*T. atomaria*, *P. pavonica*, *D. dichotoma,* and *Dictyota spiralis*) on the settlement of the toxic dinoflagellate *O.* cf. *ovata* in the NW Mediterranean. An integrative approach was used to investigate both the chemical and eukaryotic compositions at the surface of each algal species combining untargeted LC-MS-based metabolomics and high throughput sequencing (18S rRNA Illumina MiSeq sequencing), respectively. Applications of dedicated experimental protocols allowed the selective extraction of the surface metabolites of each algal species (Othmani et al., 2016a) and the activity of these extracts were further tested on monocultures of the toxic dinoflagellate.

MATERIALS AND METHODS

Field sampling was performed at 9 a.m. on the 7th of July 2017 during an *O.* cf. *ovata* bloom at the Rochambeau site in the bay of Villefranche-sur-Mer (France, Ligurian Sea; 43°41′34.83″ N, 7°18′31.66″ E) known for the recurrence of such events (Cohu et al., 2013; Jauzein et al., 2018; Gémin et al., 2020). The seawater temperature and salinity were 23.9°C and 39, respectively, at the time of the collection. Thirteen specimens of each macroalgal species (*D. dichotoma*, *D. spiralis*, *P. pavonica,* and *T. atomaria*) were collected at 0.5 m depth by snorkeling. The collection of the macroalgae followed the protocol recommended by Totti et al. (2010) and consisted in holding specimens of each species with zip bags avoiding any agitation of the surrounding seawater and resuspension of benthic cells, followed by a careful removing of their holdfast from the rocky substrate using tweezers. All zip bags containing macroalgae specimens and surrounding seawater were immediately closed underwater and processed

in the lab the same morning using: (i) four specimens of each species to measure the abundance of *O.* cf. *ovata* and diatoms at the algal surface, (ii) six specimens of each species to extract the surface and the whole macroalgal metabolomes, and (iii) three specimens of each species for the analysis of epiphytic eukaryotic communities through 18S rRNA gene high-throughput sequencing. After sampling for macroalgae, a volume of 1 L of seawater was also collected from the water column at the sampling site for 18S rRNA gene high-throughput sequencing.

Microalgal Cell Abundance at the Surface of the Macroalgae

Four specimens of each macroalga were transferred from their zip bag to 15 mL Falcon tubes filled with 4 mL of filtered seawater (0.2 μm) and 150 μL of acidic Lugol's iodine solution. The tubes were vigorously shaken and then vortexed during 5 s to remove epiphytes. Supernatants were kept in the Falcon tubes while the macroalgal thalli were removed with tweezers and air-dried on a filter paper. No pre-filtration of the supernatant was needed (Totti et al., 2010) as sediments were not abundant. Pictures of the macroalgae were taken to further estimate their surface area using the Mesurim® software and to allow the expression of the cell abundance in cell cm^{-2}. Epiphytic cell abundances in the rinsed water were determined in a 1 mL volume Sedgwick Rafter counting chamber under an inverted phase contrast microscope (Zeiss Axiovert 40C) at a magnification of ×40. Identification of diatoms and dinoflagellates was performed using data from the literature (Bertalot et al., 2000; Horiguchi, 2014, respectively).

Chemical Extraction and Analysis of Macroalgal Samples

The surface metabolome of the four seaweed species was investigated on six replicates by a dipping method previously developed for *T. atomaria* (Othmani et al., 2016a) that caused no disruption of its membranes. *P. pavonica* is expected to have similar membrane strength as its surface is calcified (Benita et al., 2018). The integrity of the cell walls of the two softer *Dictyota* species was confirmed after soaking using an optical microscope. Briefly, surface extracts (SEs) were obtained by soaking each algal thallus during 5s in an 8 mL glass vial filled with 5 mL of methanol (MeOH). The total extracts (TEs) were obtained by soaking each thallus in 7 mL of MeOH during 18 h. Both resulting extracts (SEs and TEs) were concentrated under reduced pressure and stored at −20°C until analyses and bioassays. The approximate extracted surface area of each thallus was measured therefore leading to an estimation of the amount of extracts per cm^2 of macroalga (**Table 1**).

DNA Extraction and Amplification of the Epiphytic Communities

The epiphytic microbiota was sampled using a sterile scalpel, introduced into plastic Eppendorf tubes (2 mL) and flash frozen in liquid nitrogen. DNA extraction was carried out using the PowerBiofilm DNA isolation Kit (Qiagen) and samples were preserved at −80°C. After DNA extraction, the V7 region of 18S rRNA gene was amplified using 960F and NSR1438R primers following Debroas et al. (2017). Amplicons were sent to GeT Platform (Toulouse, France) for MiSeq Illumina sequencing (2 × 250 bp).

18S rRNA Gene Metabarcoding Data Processing and Analysis

18S rRNA gene reads were processed using the FROGS workflow under Galaxy environment (Escudié et al., 2017). Sequences were quality filtered by removing those for which primers sequences were not present. The primer search accepts 10% of differences. Primers sequences were then removed in the remaining sequence using "cutadapt." Clustering step was performed using SWARM with a clustering aggregation distance set to 3 (Mahé et al., 2014). Chimeric sequences were removed *de novo* using VSEARCH (Rognes et al., 2016). Rare OTUs representing less than 0.005% of all sequences were removed. OTUs were affiliated with the Silva 132 18S rRNA. The final matrix was obtained by performing a rarefaction to the minimum library size (8975 reads) using the "phyloseq" R package (McMurdie and Holmes, 2013). Eukaryotic β-diversity was analyzed with a non-metric multidimensional scaling (NMDS) using Jaccard distances with the "phyloseq" package (McMurdie and Holmes, 2013). PERMANOVA test was performed using the distance matrix constructed with the Jaccard index, using the "vegan" R package (Oksanen et al., 2013).

Bioassays

A bioassay was designed to test the activity of the SEs in 48-well plates for which the well surface is ∼1 cm^2. The low amounts of SEs available (0.2–5 mg) allowed only one bioassay. The activity of compounds of the SEs being unknown, the highest concentrations prepared from the SEs were tested to ensure a biological response: 2.5, 3.5, 1, and 2 mg cm^{-2} for *T. atomaria*, *P. pavonica*, *D. dichotoma,* and *D. spiralis*, respectively. These concentrations are higher than those naturally encountered at the surface of the macroalgae by a factor 5, 4, 1, and 3, respectively (**Table 1**). All SEs were re-suspended in dimethyl sulfoxide (DMSO) to reach concentrations of 50, 70, 20, and 40 mg mL^{-1}, respectively for each alga. A volume of 50 μL of each SE was added to the wells containing a thin layer of fresh unsolidified agar and further dried at room temperature (0.3% of DMSO final volume). A same volume of DMSO was similarly added to six more wells as a control.

A monoclonal strain of *O.* cf. *ovata* obtained from the MCCV (Mediterranean Culture Collection of Villefranche, MCCV054) was grown in L1 medium (Guillard and Ryther, 1962) prepared with autoclaved aged and filtered seawater (from the Bay of Villefranche), adjusted to a salinity of 38 and maintained at 24°C under a 14:10 light/dark cycle with a light intensity of 250 μmol m^{-2} s^{-1}. After four days of growth (early exponential phase), 2 mL of the microalgal culture were sampled and fixed with acidic Lugol's iodine solution (4% v/v) and the cell abundance was determined using a Sedgwick rafter counting chamber and an inverted phase contrast microscope (Zeiss Axiovert 40C) at a magnification of ×40. Appropriate volumes of culture and L1

TABLE 1 | Mean concentration (mg cm^{-2}) of the SEs obtained from each macroalgal species given with the mean surface area measured for each species (n = 4).

Species	Natural concentration		Tested concentration		Macroalgal surface	
	Mean mg cm^{-2}	SD	Concentration mg cm^{-2}	Enrichment factor	Mean cm^2	SD
Taonia atomaria	0.5	0.1	2.5	5	7.4	1.8
Padina pavonica	0.9	0.3	3.5	4	7.3	2.3
Dictyota dichotoma	0.8	0.2	1.0	1	2.5	1.8
Dictyota spiralis	0.7	0.1	2.0	3	6.0	2.3

The concentration of the SEs tested in the bioassays is also given together with an estimation of the enrichment factors compared to natural concentrations. The enrichment factor was calculated as follow: Enrichment factor = Concentration $\left(\frac{\text{tested}}{\text{natural}}\right)$.

medium were added to each well previously filled with SEs or DMSO (blank) to obtain a concentration of 100 cell mL^{-1} of *O.* cf. *ovata* cells with a final volume of 1.4 mL. All well plates were incubated 24 h in the same conditions as for the cultures.

To monitor the bioactivity of the SEs on *O.* cf. *ovata*, both the physiological state and the abundance of the cells were measured after 24 h of incubation. All well plates were placed in the dark for 15 min and the well content are successively transferred to a 2 mL glass cuvette immediately moved to a MC-PAM (Multi-Color Pulse-Amplitude-Modulated, Heinz Walz Gmbh, Effeltrich, Germany) equipped with a blue LED (440 nm) as a source for the actinic light and a white LED used for the saturating pulses. The maximum quantum yield (F_v/F_m) of the photosystem II (PSII) was used as a proxy of the microalga physiological state. It was calculated as $(F_m - F_0)/F_m$, where F_0 is the fluorescence of a dark-adapted sample and F_m is measured after application of a saturation pulse of light (intensity 431 $\mu E\ m^{-2}\ s^{-1}$, 300 ms duration). Curve-fitting software provided with the instrument (PAMwin V3.20W) was used to obtain F_v/F_m. All curve fits and fluorescence transients were manually inspected in real time. Each sample was placed back in its well after the PAM measurement and immediately fixed with acidic Lugol's iodine solution (4% v/v) for cell counting under microscope as described earlier. The growth rate of *O.* cf. *ovata* was calculated for each well as follows:

$$\mu = \frac{\ln(N2/N1)}{t2 - t1}$$

where N1 and N2 are the cell abundances at times t1 (beginning of the experiment) and t2 (sampling after 24 h).

UHPLC-HRMS Analysis of Macroalgal Extracts

Before injection, samples were solubilized in 1 mL of LC-MS grade MeOH. Eleven quality control samples (QCs) and four analytical blanks were also prepared as described in Paix et al. (2020), and all samples were randomly injected to avoid systematic errors. Acquisition was performed by UHPLC-HRMS using a Dionex Ultimate 3000 rapid Separation chromatographic system (Thermo Fisher Scientific, Waltham, MA, United States) coupled to a QToF Impact II mass spectrometer (Bruker Daltonics, Bremen, Germany) equipped with an electrospray source. A volume of 5 µL of each sample was injected and analyzed on a reversed phase column (150 × 2.1 mm, 1.7 µm, Kinetex Phenyl-Hexyl equipped with a SecurityGuard cartridge; Phenomenex, Le Pecq, France) with a column temperature of 40°C and a flow rate of 0.5 mL min^{-1}. Mobile phases were (A) water and (B) acetonitrile (Chromasolv; Sigma-Aldrich-Merck, Darmstadt, Germany) containing each 0.1% (v/v) of formic acid (Ultra grade; Fluka, Fischer Scientific, Illkirch, France). The elution gradient started at 5% B and kept for 2 min, then to 100% B (linear ramp) in 8 min and kept for 4 min; then back to 5% B (linear ramp) over 0.01 min and maintained 1.99 min, for a total run time of 16 min. Mass spectrometry (MS) analyses were performed in the full scan positive mode (ESI+). The capillary voltage of the MS spectrometer was set at 4500 V and the nebulizing parameters were set as follows: nebulizing gas (N_2) pressure at 0.4 bar, drying gas (N_2) flow at 4 L min^{-1}, and drying temperature at 180°C. Mass spectra were recorded from m/z 50 to 1200. Tandem mass spectrometry analyses were performed with a collision induced dissociation (CID) and collision energy of 25 eV. A solution of formate/acetate forming clusters was automatically injected before each sample for internal mass calibration, and the mass spectrometer was calibrated with the same solution before each sequence of samples. Raw UHPLC-HRMS data were analyzed using DataAnalysis (version 4.3; Bruker Daltonics), converted into netCDF files and processed for peak finding, integration and alignment using the open source XCMS package (version 1.46.0; Smith et al., 2006) in the R 3.2.3 environment. The resulting variables list was filtered using three successive steps (signal/noise ratio, coefficient of variation and coefficient of autocorrelation) with an in-house script running on R. These variables were $\log_{10}$-transformed, mean-centerd and normalized using the sum of the chromatographic peak areas as described in Paix et al. (2020), and analyzed by Principal Component Analysis (PCA) and partial least-square discriminant analysis (PLS-DA) using the MetaboAnalyst 3.5 online resource[1]. The global annotation was assessed by comparison of MS/MS spectra with those of an in-house database (purified compounds and commercial standards), and public databases (MarinLit, MetLin, MoNA, or Lipidmaps). Subsequently, the annotation procedure of analogs of known compounds was facilitated by molecular networking using the GNPS platform[2].

[1]http://www.metaboanalyst.ca

[2]https://gnps.ucsd.edu/ProteoSAFe/static/gnps-splash.jsp

RESULTS

Assessment of the Natural Abundance of Benthic Microalgae Using Microscopy

All four macroalgal species had their surface colonized by diatoms, including species of the genera *Licmophora*, *Amphora*., *Navicula*, *Cylindrotheca*, *Striatella,* and *Gyrosigma*, as well as the dinoflagellate *O.* cf. *ovata* (**Figure 1**). *O.* cf. *ovata* showed a lower abundance than diatoms, representing 14–23% of the total number of counted cells, with densities ranging from 1.5 to 7.9 $\times$ 10^3 cell cm^{-2}. Significant different concentrations of *O.* cf. *ovata* cells were observed between macroalgal hosts (ANOVA: $p = 0.0175$). *Post hoc* analysis revealed a significantly higher concentration of cells on *D. dichotoma* compared to *D. spiralis* and *P. pavonica*, while no significant differences were detected between *T. atomaria*, *P. pavonica,* and *D. spiralis*, and neither between *T. atomaria* and *D. dichotoma* – due to one outlier sample.

Diversity of Epiphytic Eukaryotes Through 18S rRNA Gene HTS

When compared to the number of OTUs, the Chao1 index reflects the richness that could be reached if a higher number of sequences has been obtained. Here, Chao1 indicated that the highest richness of eukaryotic communities was observed in seawater as well as on the surface of *T. atomaria* and *P. pavonica* (**Supplementary Figure S1**). Considering the β-diversity, seawater communities were clearly dissimilar from those found on the macroalgal surfaces (**Figure 2** and **Supplementary Figure S2**). The dinobiontes seemed to constitute the major taxa in seawater, with *Amphidinium* being the most represented genus (54%) followed by *Alexandrium* (9%), while *Ostreopsis* only represented 3%. Among epiphytes, a clear clustering at the algal species level could be noticed, with the two *Dictyota* species communities on the one hand, and *T. atomaria* and *P. pavonica* communities on the other hand (**Supplementary Figure S2**). Using the Jaccard index with a NMDS analysis, the β-diversity of the eukaryotic communities revealed clear differences between the epiphytic and the planktonic communities, but also between macroalgal hosts (**Figure 2** and **Supplementary Figure S2**, PERMANOVA: $p = 0.001$).

Even though they serve as support of common taxa, like Dinoflagellata, Arthropoda, Ochrophyta, Annelida, Florideophycideae, and Mollusca, the four macroalgae species exhibited a contrasted composition of their epiphytic eukaryotic communities. Among the major detected taxa, two belonged to microalgae (Ochrophyta and Dinoflagellata), one to copepods (Arthropoda), two to red algae (Florideophycideae) and two to upper benthic organisms (Annelida and Mollusca). The major species of diatoms present on the macroalgae belonged to the genera *Berkeleya*, *Navicula*, *Haslea*, *Nitzschia*, *Actinocyclus*, *Amphora*, *Cylindrotheca*, *Cocconeis*, *Psammoneis*, *Hyalosira,* and *Frustulia* and their relative abundance was the highest on *P. pavonica* (19%) and the lowest on *D. spiralis* (2%). The abundance of Dinoflagellata in the epiphytic community determined by cell counting was highly consistent with the results obtained by 18S rDNA gene sequencing. The major OTU identified belonged to the genus *Ostreopsis*, while other dinoflagellate taxa, without specific affiliation at the genus level, were also detected with very few sequences. Dinoflagellates represented only 1% of the total eukaryotic diversity on *T. atomaria*, *P. pavonica,* and *D. spiralis* while it reached 6% on *D. dichotoma*. The Harpacticoids, Amphiascoides, and Paramphiascella were the main Arthropoda families and the species *Amonardia coreana*, *Parastenhelia* sp., *Amphiascoides atopus,* and *Paramphiascella fulvofasciata* were annotated. Several Annelida species of the Phyllodocida family were detected, including *Platynereis dumerilii* and *Syllis pigmentata*; they were mainly distributed on *D. dichotoma* and *P. pavonica*. The major platyhelminthe species was *Convoluta convoluta* which was reported on the two *Dictyota* spp. The Arthropoda were particularly represented on *D. spiralis* (67%) and *T. atomaria* (32.5%) while *P. pavonica* showed the highest Annelida community (39.5%). The Florideophycideae also largely contributed to the eukaryotic diversity on *T. atomaria* (22.4%). These same taxa were shown to colonize *D. dichotoma*, none of them being predominant: Dinoflagellata (6%), Arthropoda (18%), Ochrophyta (10%), Annelida (23%), Florideophycideae (12%), Mollusca (8%), and Xenacoelomorpha (16%).

Chemical Analysis of Macroalgal Extracts

The chemical diversity of the four macroalgal extracts was assessed by untargeted LC-MS-based metabolomics and led to 375 features after filtering. The PCA score plot of the surface and total (SEs and TEs) macroalgal extracts (**Figure 3**) showed a clear separation between the two *Dictyota* spp. and the two other species (*T. atomaria* and *P. pavonica*), mainly on the first component (48% of the total variance) highlighting a distinct chemical composition between these species. Furthermore, the second component (18.5% of the total variance) highlighted differences between SEs and TEs within each of these two algal groups. A list of the features responsible for the differences between SEs and TEs for each species is provided in **Supplementary Table S1**. The vast majority of these metabolites being minor ions on the chromatograms, very few could be annotated. Most metabolites specific to the SEs were small/polar compounds as suggested by their retention time (RT $<$ 1 min) whereas TEs were more enriched in less polar metabolites (RT $>$ 8 min). Dimethylsulfoniopropionate (DMSP), *Lyso*-diacylglyceryl-3-*O*-carboxyhydroxymethylcholine (C16:0) and a compound, putatively annotated as acetyl-*L*-cysteine, were found to be enriched in the SEs of *T. atomaria, P. pavonica,* and *D. dichotoma*, respectively.

The score plot of the PLS-DA only built with SEs (**Figure 4**) offered a more focused view of the distribution of these extracts. None of the SEs overlapped with 95% confidence, suggesting significant differences in their chemical content, even for the two *Dictyota* spp. The distribution of the samples on both the PCA and the PLS-DA score plots was highly driven by the large number of metabolites produced by *D. dichotoma* and *D. spiralis*.

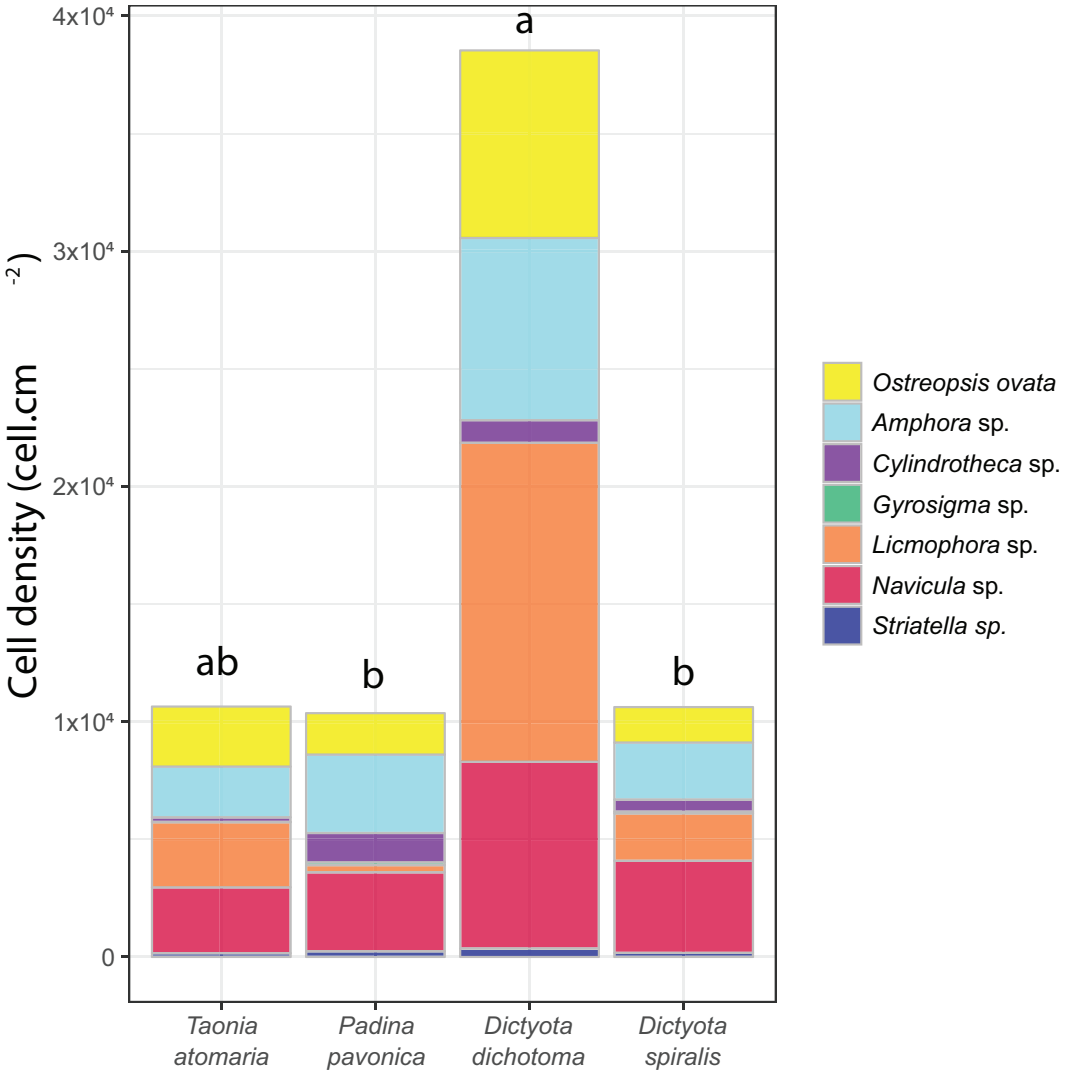

FIGURE 1 | Cell density (cell cm^{-2}) of major diatoms and *O.* cf. *ovata* at the surface of the four macroalgae. Statistical significance was evaluated only for *O.* cf. *ovata* abundances using an ANOVA test (*p = 0.0175) followed by a *post hoc* Tukey's test (results indicated by a,b indexes).

The first 50 Variable Importance of Projection (VIPs) responsible for the separation of the samples on the PLS-DA score plot (VIP score >1.1) are listed in **Table 2**.

The Search of matches of MS data from compounds of our in-house database, the MarinLit database and molecular network built from MS/MS spectra analysis (**Figure 5**) allowed the annotation of several of the VIPs characteristic of each macroalga (**Table 2**).

Several chemical markers enriched in *D. dichotoma* and *D. spiralis* SEs were detected in cluster B and I of the molecular network, allowing their putative annotation as diterpene derivatives. More precisely, the diterpenes dictyotalide A (or an isomer) (VIP n°4), *ent*-erogorgiaene (VIP n°10), dictyotetraene (VIP n°14), dictyol A (VIP n°15), isopachydictyol A (VIP n°19), 17,18-18,19-bisepoxyxenic-19-methoxy-6,9,13-triene (VIP n°25) and tricyclodictyofuran C (VIP n°6 and 41) were putatively identified in cluster B, and dictyotadimer A (VIP n°13) in cluster I. Finally, even if not appearing in the molecular network, dictyol B (VIP n°29) was also putatively annotated. Several other VIPs were not identified but were characterized as diterpenes or diterpene derivatives using their MS and MS/MS data.

Both the lipid geranylgeranylglycerol and the sulfur compound DMSP (VIPs n°20 and 27, respectively) were identified by the mean of chemical standards as the major markers found in *T. atomaria* SEs. Five other compounds (VIPS n°31, 36, 37, 40, and 42), putatively identified as diacylglyceryl-3-*O*-carboxyhydroxymethylcholines [DGCCs (C22:6), (C44:12), (C36:6); *Lyso*-DGCCs (C16:0), and (C38:6), respectively), were also detected in *T. atomaria* and gathered in cluster D. Finally, the VIP n°46 was putatively annotated as the sesquiterpene *trans*-calamenene using an in-house standard.

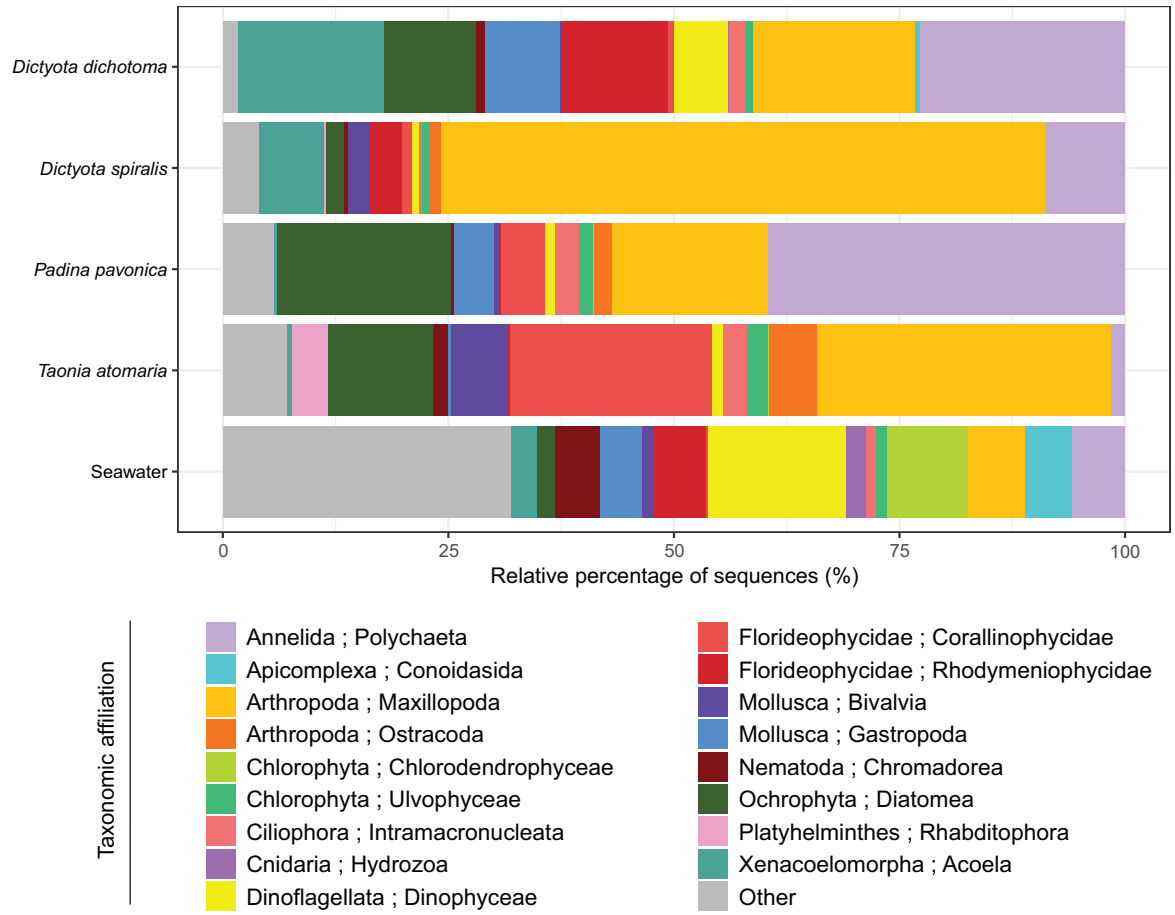

FIGURE 2 | Eukaryotic communities colonizing the surface of the four macroalgae and present in the surrounding seawater. Replicate samples of a same species were averaged (n = 3) and relative colonization to all sequences is given (%). Taxonomic affiliation corresponds to the Phylum and Class level. "Other" combines Classes that represent less than 2% of the total diversity.

Padina pavonica was the algal species that showed the least chemical richness on its surface with only two unidentified markers (VIPs n°34 and 49) being found in its corresponding SEs.

More compounds not listed as VIPs were identified from other clusters of the molecular network: diacylglycerylhydroxymethyl-*N*,*N*,*N*-trimethyl-β-alanines (DGTAs) and phosphatidylcholines (PCs) present in cluster A, other PCs in cluster E, carotenoids in cluster F, sesquiterpenoids in cluster G, and pheophytin a derivatives in cluster N.

Bioactivity of Surface Extracts on *O.* cf. *ovata*

To ensure a measurable effect on *O.* cf. *ovata* cells, the maximal concentration that could be obtained from the SEs was tested for their bioactivity. Therefore, tested concentrations varied from 1 to 3.5 mg cm^{-2} according to the species and comparison between bioactivities should be treated cautiously. Three macroalgal SEs out of four induced a significant growth reduction of *O.* cf. *ovata* ($p < 0.001$; **Figure 6A**), with *D. spiralis* SE found to be not statistically active. Despite tested at the lowest concentration (1 mg cm^{-2}), the inhibition of *O.* cf. *ovata* growth induced by *D. dichotoma* SEs was similar to those of *P. pavonica* while being significantly lower than the one of *T. atomaria*. Although similar concentrations were used for *T. atomaria* and *D. spiralis* SEs (2.5 and 2 mg cm^{-2}, respectively), the inhibition on *O.* cf. *ovata* growth induced by *T. atomaria* SEs was significantly higher.

All but *P. pavonica* macroalgal SEs induced a significant stress on *O.* cf. *ovata* physiology as conveyed by the significant alteration of the efficiency of the PSII shown by the Fv/Fm ratio ($p < 0.001$; **Figure 6B**). Despite being tested at the lowest concentration, the SEs of *D. dichotoma* caused among the most intense inhibition of the PSII efficiency. Such an inhibition was comparable to those observed for *D. spiralis* and *T. atomaria* SEs. Whether the growth rate of *O.* cf. *ovata* was not affected by *D. spiralis*, the PSII efficiency was significantly altered to a similar extent than with *D. dichotoma*. Mirroring the effects on *O.* cf. *ovata* growth rate, *T. atomaria* SEs tested at 2.5 mg cm^{-2} also caused an intense stress on the PSII of the dinoflagellate. The related reduction in the Fv/Fm ratio measured was significantly higher than for *D. spiralis* and *P. pavonica*, although tested at a similar and lower concentration, respectively.

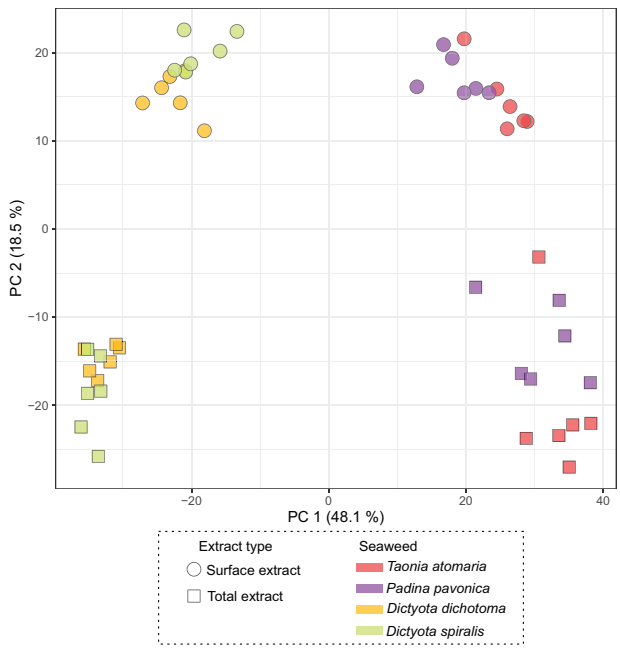

FIGURE 3 | PCA score plot obtained from LC-(+)-ESI-MS metabolomics analyses of both the total extracts (TEs) and surface extracts (SEs) of the four macroalgae.

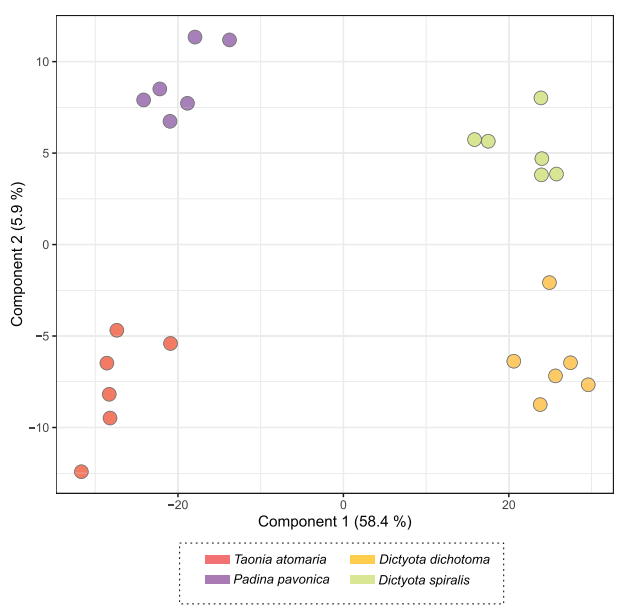

FIGURE 4 | PLS-DA score plot obtained from LC-(+)-ESI-MS metabolomics analyses of the surface extracts (SEs) of the four macroalgae.

DISCUSSION

The simultaneous monitoring of both the abundance and toxin content of benthic *O.* cf. *ovata* cells undertaken by Gémin et al. (2020) at the same sampling site in the bay of Villefranche showed that the development of this bloom followed a classic trend. In terms of intensity, the bloom peaked at 9.2 ± 7.5 10^5 cells g^{-1} FW (Gémin et al., 2020) corresponding to a moderate bloom for this site (Guidi-Guilvard et al., 2012; Cohu et al., 2013) or other Mediterranean sampling sites (Totti et al., 2010). Consistently with our results but also with other observations from the NW Mediterranean Sea (Cohu et al., 2013; Blanfuné et al., 2015), Gémin et al. (2020) found the highest cell concentration of *O.* cf. *ovata* on *Dictyota* spp. and the lowest on *P. pavonica*.

Potential Control of the Abundance of *O. cf. ovata* by the Epiphytic Community

A preferred colonization by *O.* cf. *ovata* on branched, three-dimensional thalli with a high surface/volume ratio has been previously suggested by several authors (Vila et al., 2001; Totti et al., 2010; Gémin et al., 2020) but such an hypothesis is not fully supported by the low abundance of *O.* cf. *ovata* measured on the highly branched *T. atomaria* or by settlement differences observed between morphologically similar *Dictyota* species (this study and Blanfuné et al., 2015). The 18S rRNA gene sequencing revealed a high diversity of eukaryotes colonizing the macroalgae, suggesting that various biotic interactions may take place within the epiphytic community having the potential to regulate the colonization of *O.* cf. *ovata*.

Inter-specific competition for nutrients, light and space may occur between the dinoflagellate *O.* cf. *ovata* and the various species of diatoms that co-occurred within the epiphytes of the macroalgae. Species of the genera *Licmophora*, *Navicula*, and *Amphora* were the most abundant diatoms co-occurring with *O.* cf. *ovata*, in line with previous findings (Accoroni et al., 2016), while *Coscinodiscus* spp. usually detected in the Catalan Sea (Vila et al., 2001; Carnicer et al., 2015) was missing. Other dinoflagellate species were barely detectable conversely to previous studies that reported the co-occurrence of *P. lima* and *C. monotis* in various sampling sites across the Mediterranean Sea, including the bay of Villefranche (Vila et al., 2001; Aligizaki and Nikolaidis, 2006; Cohu et al., 2011; Blanfuné et al., 2015; Accoroni et al., 2016). In recent co-culture experiments, weak deleterious allelopathic effects induced by *Licmophora paradoxa* toward *O.* cf. *ovata* were highlighted (Ternon et al., 2018). A chemical control of the colonization of *O.* cf. *ovata* by co-occurring benthic microalgae is therefore possible although it may be counterbalanced by the existence of an additional weak inhibiting allelopathic effects applied by *O.* cf. *ovata* on co-occurring microalgae (Monti and Cecchin, 2012; García-Portela et al., 2016).

Predation by benthic copepods is another factor that may modulate the colonization pattern of benthic microalgae. Benthic harpacticoids, such as *Sphaeroma serratum*, *Tigriopus fulvus*, *Acartia clausi*, and *Sarsamphiascus* cf. *propinquus*, have been recently shown to feed on *O.* cf. *ovata* (Prato et al., 2011; Faimali et al., 2012; Furlan et al., 2013; Pavaux et al., 2019) with similar ingestion rates as for diatoms (Boisnoir et al., 2020). The resistance of benthic copepods to *O.* cf. *ovata*'s toxicity was found to be highly variable among species, with LC_{50} ranging from 10 to 20,000 cells mL^{-1} (Prato et al., 2011; Faimali et al., 2012; Pavaux et al., 2019). Ingestion of *O.* cf. *ovata* leads to

TABLE 2 | Putative annotation of the first 50 chemical markers (VIP score >1.1) driving the distribution of the samples on the PLS-DA score plot obtained from LC-(+)-ESI-MS metabolomics analyses of the SEs of the four macroalgae.

VIP	Cluster	*m/z*	Annotation	Formula	err	msigma	*D. dichotoma*	*D. spiralis*	*P. pavonica*	*T. atomaria*	Color code
1	–	472.236753	Unknown	$C_{26}H_{34}NO_7$	−9.6	9.5					−4
2	–	390.263585	Diterpene derivative (methoxylated and acetylated)?	$C_{23}H_{36}NO_4$	−2.8	1.1					−2
3	SL	461.300916	Unknown	$C_{26}H_{41}N_2O_5$	1.0	13.0					0
4	B	319.226939	Dictyotalide A or isomer	$C_{20}H_{31}O_3$	−1.0	12.9					2
5	J	447.285584	Unknown	$C_{25}H_{39}N_2O_5$	−0.6	6.7					4
6	–	317.247489	Tricyclodictyofuran C or isomer	$C_{21}H_{33}O_2$	−1.2	12.4					
7	–	422.254062	Diterpene derivative (methoxylated and acetylated)?	$C_{23}H_{36}NO_6$	−1.6	4.6					
8	I	378.264217	Diterpene derivative (acetylated)	$C_{22}H_{36}NO_4$	−3.8	9.3					
9	–	364.284964	Diterpene derivative (acetylated)	$C_{22}H_{38}NO_3$	−2.7	17.0					
10	B	271.242119	*ent*-erogorgiaene	$C_{20}H_{31}$	−1.0	4.4					
11	–	342.242938	4-methylaminoacarone	$C_{22}H_{32}NO_2$	−2.7	11.9					
12	–	573.466831	Carotenoid (pirardixanthin derivative?)	$C_{40}H_{61}O_2$	−0.3	28.1					
13	I	637.448128	Dictyotadimer A	$C_{40}H_{61}O_6$	−2.7	14.0					
14	B	269.226492	Dictyotetraene	$C_{20}H_{29}$	−0.3	66.9					
15	B	285.221393	Dictyol A*	$C_{20}H_{29}O$	−1.8	12.4					
16	–	413.280297	*Apo*-carotenoid	$C_{30}H_{37}O$	8.5	4.4					
17	B	283.20567	Unknown	$C_{20}H_{27}O$	−1.0	7.9					
18	–	743.450601	Unknown	$C_{46}H_{63}O_8$	−1.0	38.4					
19	B	289.252582	Isopachydictyol A or dollabellatrienone	$C_{20}H_{33}O$	0.5	6.7					
20	–	382.331504	Geranylgeranylglycerol*	$C_{23}H_{44}NO_3$	−1.7	6.1					
21	–	373.235224	Unknown	$C_{21}H_{34}NaO_4$	−0.3	2.6					
22	–	410.290343	Diterpene derivative (methoxylated and acetylated)?	$C_{23}H_{40}NO_5$	−3.4	4.7					
23	(B)	333.242627	Diterpene derivative (methoxylated)	$C_{21}H_{33}O_3$	−1.8	7.7					
24	SL	446.290738	Pharmacin B	$C_{26}H_{40}NO_5$	−1.0	7.2					
25	B	333.242496	Diterpene derivative (methoxylated)	$C_{21}H_{33}O_3$	−0.8	4.4					
26	–	406.258778	Diterpene derivative (methoxylated and acetylated)?	$C_{23}H_{36}NO_5$	−2.9	5.0					
27	–	135.047248	DMSP*	$C_5H_{11}O_2S$	0.2	1.0					

(Continued)

TABLE 2 | Continued

VIP	Cluster	*m/z*	Annotation	Formula	err	msigma	*D. dichotoma*	*D. spiralis*	*P. pavonica*	*T. atomaria*
28	–	489.343493	Unknown	$C_{26}H_{49}O_8$	−3.5	13.7				
29	—	327.229615	Dictyol B	$C_{20}H_{32}NaO_2$	−0.5	14.2				
30	–	654.47347	Carotenoid	$C_{40}H_{64}NO_6$	−5.5	18.9				
31	D	562.374243	DGCC (C22:6)	$C_{32}H_{52}NO_7$	−2.3	1.4				
32	–	356.25884	Unknown	$C_{23}H_{34}NO_2$	−2.7	16.0				
33	–	426.231272	Unknown	$C_{22}H_{36}NO_5S$	−2.6	15.7				
34	SL	653.297738	Unknown	$C_{29}H_{49}O_{16}$	2.3	10.3				
35	E	741.614801	Unknown	$C_{46}H_{81}N_2O_5$	−2.5	9.7				
36	D	872.605027	DGCC (C44:12)	$C_{54}H_{82}NO_8$	−3.1	2.1				
37	D	772.573549	DGCC (C36:6)	$C_{46}H_{78}NO_8$	−2.7	2.1				
38	–	317.247669	Tricyclodictyofuran C or isomer	$C_{21}H_{33}O_2$	−3.0	3.5				
39	SL	318.242795	Unknown	$C_{20}H_{32}NO_2$	−1.6	18.5				
40	D	490.374196	*Lyso*-DGCC (C16:0)	$C_{26}H_{52}NO_7$	−0.7	14.3				
41	B	287.237035	Tricyclodictyofuran B	$C_{20}H_{31}O$	−0.8	27.2				
42	D	800.604167	DGCC (C38:6)	$C_{48}H_{82}NO_8$	−2.1	6.6				
43	B	343.226662	Diterpene derivative (acetylated)	$C_{22}H_{31}O_3$	−2.2	9.6				
44	SL	260.112865	Unknown	$C_{11}H_{18}NO_6$	−0.6	3.2				
45	–	453.27291	*Apo*-carotenoid	$C_{30}H_{38}NaO_2$	4.0	10.3				
46	–	201.16362	*Trans*-calamenene*	$C_{15}H_{21}$	−2.8	25.8				
47	SL	376.787236	FA (C24:5)	$C_{24}H_{42}NO_2$	3.3	9.9				
48	SL	445.292694	Amphidinolide	$C_{25}H_{42}NaO_5$	−0.1	5.3				
49	–	704.546719	Unknown	$C_{42}H_{74}NO_7$	−2.5	7.7				
50	–	319.226828	Dictyotalide A or isomer	$C_{20}H_{31}O_3$	−0.3	27.0				

*Identification of the compounds marked by * was confirmed with a chemical standard. Clusters "SL" corresponds to a self-loop (a metabolite only connected to itself). The color code represents the mean concentration values obtained for each macroalga. DGCC, diacylglyceryl-3-O-carboxyhydroxymethylcholines; FA, fatty acid.*

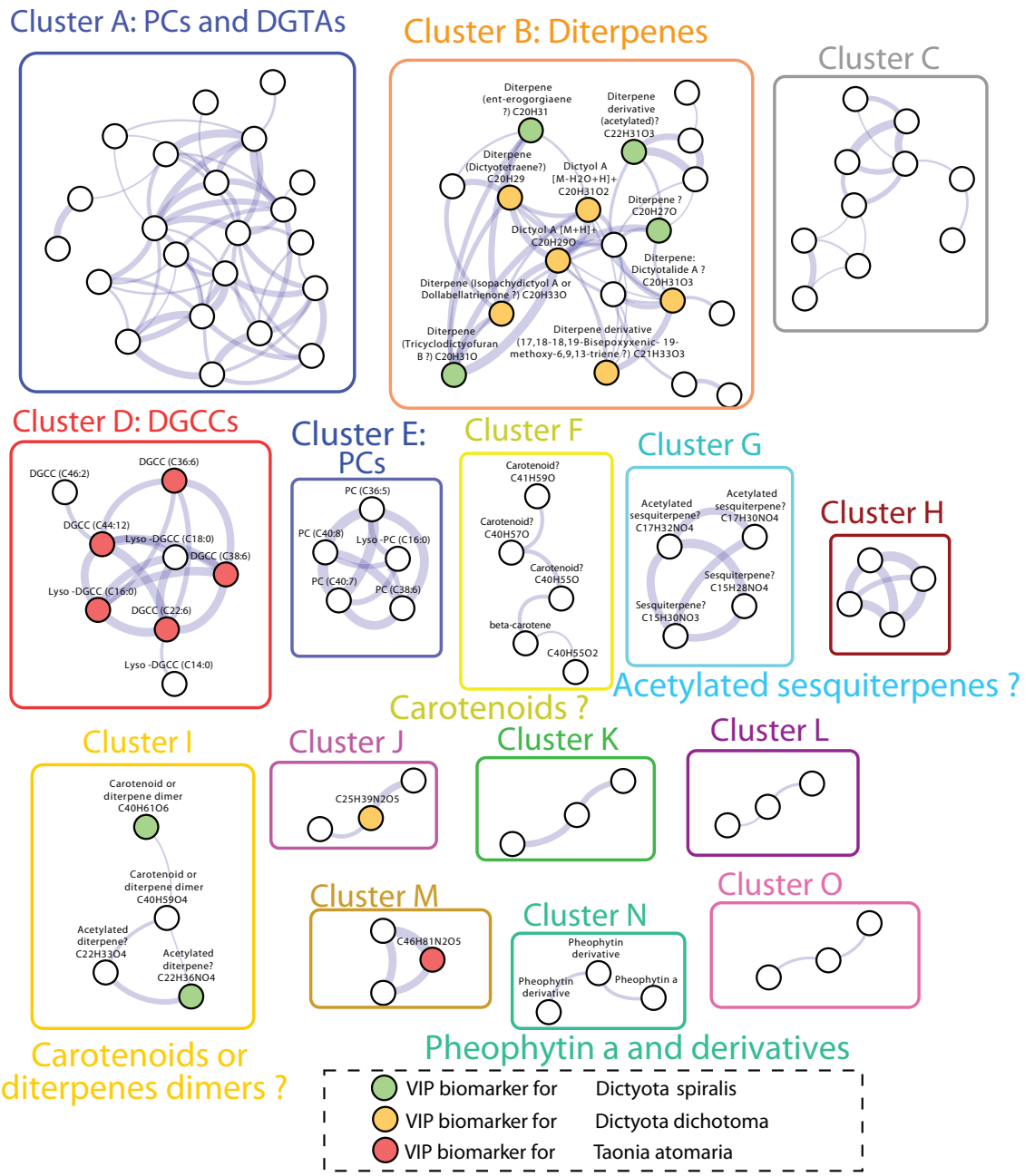

FIGURE 5 | Molecular network obtained from LC-(+)-ESI-MS/MS data of the SEs of the four macroalgal species. Only clusters with three or more nodes are represented. Nodes represent MS/MS spectra which are connected based on their spectral similarity. Colored nodes indicate biomarkers according to the four macroalgae (orange: *D. dichotoma*, green: *D. spiralis*, red: *T. atomaria*, no VIPs for *P. pavonica* were observed). The edge width is proportional to the cosine score. PC, phosphatidylcholines; DGTA, diacylglycerylhydroxymethyl-N,N,N-trimethyl-b-alanines; DGCC,diacylglyceryl-3-*O*-carboxyhydroxymethylcholines.

reduced fecal pellets production and fecundity rates indicating a reprotoxic effect (Pavaux et al., 2019) that may cause a reduction in nauplii abundance (Guidi-Guilvard et al., 2012) but not on adults' abundance. Our study was conducted at the peak of the bloom, when the highest concentrations of O. cf. *ovata* and toxin content per cell were reported (Gémin et al., 2020). *In situ* cell concentrations reported in cells per g of macroalga fresh weight ($9.2 \pm 7.5\ 10^5$ cells g^{-1} FW; Gémin et al., 2020) likely exceeded the toxic level of 20,000 cells per mL (Pavaux et al., 2019). Nevertheless, the amount of toxins per cell reported *in situ* was lower compared to the MCCV054 strain of *O.* cf. *ovata* used in Pavaux et al. study (5–10 against 13 pg $cell^{-1}$; Gémin et al., 2020; Pavaux et al., 2020, respectively). Additionally, Gémin et al. (2020) showed that the toxin content in *O.* cf. *ovata* varied

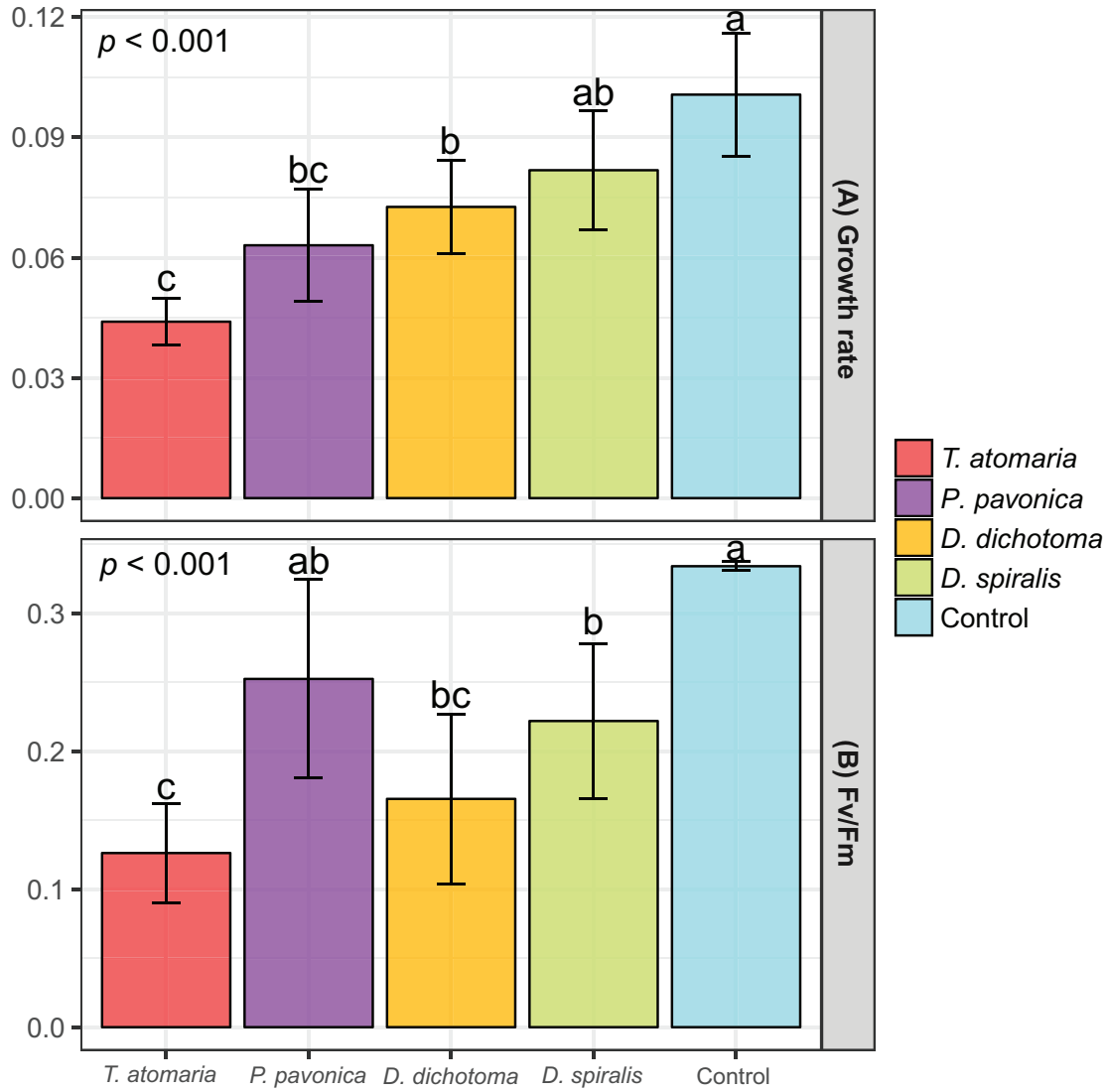

FIGURE 6 | (A) Growth rate (μ) of *O.* cf. *ovata* and **(B)** Maximum quantum yield of PSII (F_v/F_m) of dark-adapted samples of *O.* cf. *ovata* after exposure of 24 h to macroalgal surface extracts (SEs) and blanks (n = 6 per condition). p-values and a, b, c indexes correspond to results of the one-way ANOVA and Tukey's tests, respectively.

according to the macroalgal species they colonized. The toxicity of *O.* cf. *ovata* toward grazers may therefore vary according to the substrate. Therefore, it is difficult to conclude whether the maxillopods are suffering from the natural concentrations of *O.* cf. *ovata* encountered on the four macroalgae. Moreover, the resistance of the copepod species (*P. fulvofasciata*, *A. atopus*, *A. coreana*, *Harpaticus* spp., and *Nemesis* spp.) detected on the four macroalgae to *O.* cf. *ovata* has not been experimentally tested and may differ from already tested species. It is worth noting that the relative abundance of benthic copepods and *O.* cf. *ovata* did not show any obvious correlation. In contrast, if maxillopods have the capacity to feed on *O.* cf. *ovata*, they unlikely are the major factor that regulates its colonization on the macroalgae. Indeed, the toxic dinoflagellate was found to be similarly abundant on *D. spiralis*, *T. atomaria,* and *P. pavonica* (1,505; 2,251, and 1,759 cells cm^{-2}, respectively), not mirroring their different ratio *Ostreopsis*:maxillopods (1:67, 1:33, and 1:17, respectively) in term of comparison of 18S rRNA gene sequences.

Other predators, like polychaetes, were also shown to graze *O.* cf. *ovata* despite an important sensitivity to the ovatoxins (Simonini et al., 2011). Concentrations of *O.* cf. *ovata* as low as 200 cells mL^{-1} caused the death of 100% of a population of *Dinophylus gyrociliatus* in less than 48 h (Simonini et al., 2011). However, similarly to copepods, the capacity to feed on *O.* cf. *ovata* as well as the resistance to the ovatoxins may differ among species and according to the toxicity of *O.* cf. *ovata* cells linked with the substrate they colonize (Gémin et al., 2020). The species *S. pigmentata*, *P. dumerilii,* and *Neodexiospira brasiliensis,* for

which no LC_{50} is available yet, were the most abundant while *D. gyrociliatus* was not detected on the macroalgae.

The eukaryotic richness of the epiphytic macroalgal communities was high, particularly on *T. atomaria* and *P. pavonica*, and interactions that may result from it have not been fully investigated yet. For instance, the bacterial community which was not described in this study may play an important role in the regulation of epiphytic communities (Tait et al., 2005; Wheeler et al., 2006; Saha and Weinberger, 2019), including *O.* cf. *ovata*. The present data set did not highlight a specific biotic interaction within the epiphytic community that may favor or inhibit the settlement of *O.* cf. *ovata* on the different macroalgal species.

Algal Surface Chemistry Influences the Growth of *O.* cf. *ovata*

Several studies have shown deleterious effects of macroalgal metabolites on microalgae using whole cells dried and grounded (Tang and Gobler, 2011; Accoroni et al., 2015) or organic whole-cell extracts (Hellio et al., 2002; Nagayama et al., 2003). To our knowledge, this study is the first attempt in evaluating the bioactivity of SEs on settlement and growth of a microalgal species. Previous study on *T. atomaria* demonstrated a satisfying extraction of surface metabolites without disturbance of the macroalgal membranes by the soaking protocol used in the present study (Othmani et al., 2016a). The differences observed in the chemistry of the SEs and TEs for all four macroalgae species further validated the soaking protocol as an efficient method to extract surface metabolites of the three other species *P. pavonica*, *D. spiralis,* and *D. dichotoma*. Most chemical markers characteristics of the SEs were found to be polar metabolites (RT < 1 min), including DMSP, whereas TEs were characterized by less polar compounds (RT > 8 min).

The chemical fingerprint of the four macroalgae species draws two distinct groups: the two *Dictyota* spp. clustering together and *P. pavonica* and *T. atomaria* gathering in the second group. In terms of eukaryotic β-diversity, the same two groups emerged, suggesting that the metabolites at the surface of the macroalgae are influencing the settlement of eukaryotes. Since both *T. atomaria* and *P. pavonica* showed a higher richness of their overall epiphytic eukaryotic community, their surface metabolites could be considered less bioactive toward these communities, although higher antibacterial activities have been previously observed for *Taonia* and *Dictyota* spp. among Phaeophyceae species (Salvador Soler et al., 2007). When looking specifically at *O.* cf. *ovata*, the surface chemistry of the four macroalgae has the potential to influence the settlement of the toxic dinoflagellate by altering both its physiology and its growth. Nevertheless, the use of different concentrations (1–3.5 mg cm^{-2}) in the bioassay does not allow to order the bioactivity of the four macroalgae, however *D. dichotoma* clearly induced a strong inhibition of both the growth and the PSII efficiency of *O.* cf. *ovata* at ecological concentrations (1 mg cm^{-2}) and can therefore be considered as the most bioactive species. Many diterpenes isolated from *Dictyota* spp. have been found to exhibit antifouling properties as for instance the algicidal dictyolactone toward the red-tide microalgae *Heterosigma akashiwo* (Kim et al., 2006), dictyol C that reduces the adhesion of *Pseudoalteromonas* spp. (Viano et al., 2009), as well as dictyol E, dictyol B acetate, pachydictyol A and dictyodial that all cause significant larval mortalities of invertebrates (Schmitt et al., 1998). Although none of the cited compounds were major chemical markers in any of the two *Dictyota* spp., the high diterpenes content of their SEs suggests that this family of metabolites could be responsible for the observed bioactivity of both species. Nevertheless, considering the higher stress induced by *D. dichotoma* compared to *D. spiralis* on *O.* cf. *ovata*, chemical markers more specific to *D. dichotoma* were sought. Two metabolites listed as VIPs n°5 and 12 were significantly more enriched in *D. dichotoma* SEs (**Supplementary Figure S3**) with the molecular formulae $C_{25}H_{39}N_2O_5$ and $C_{40}H_{61}O_2$ corresponding to an unidentified compound (cluster J) and a carotenoid-like compound likely to belong to the pirardixanthin family (Tsushima et al., 2001), respectively. While the activity of these families of compounds has not been determined so far, some carotenoids like fucoxanthin are known to possess inhibiting properties against bacteria (Viano et al., 2009; Saha et al., 2011) which could also target benthic microalgae.

Taonia atomaria showed a higher bioactivity than *D. spiralis* and *P. pavonica*, tested at a similar and higher concentration, respectively. This bioactivity is, however, likely overestimated compared to an ecological situation (enrichment factor of 5). Both geranylgeranylglycerol and DMSP were the major biomarkers in *T. atomaria* SEs, in agreement with previous findings (Othmani et al., 2016a; Paix et al., 2019), and were therefore enriched in this species compared to the three others (**Supplementary Figure S3**). These two metabolites have shown activity against bacterial settlement (Saha et al., 2012; Othmani et al., 2016a,b) and may have the potential for inhibiting the growth of *O.* cf. *ovata*. However, DMSP is a metabolite largely biosynthesized by *O.* cf. *ovata* itself (personal data; Chen et al., 2020), leaving geranylgeranylglycerol as the most likely candidate. The present dataset did not allow to propose any metabolite for *P. pavonica* that could explain the unspecific bioactivity of its SEs. If all four macroalgae species have the ability to affect *O.* cf. *ovata*'s growth or physiology, bidirectional effects may also be considered since some macroalgae have been shown to rely on microbial metabolites for cell division and differentiation (Wichard and Beemelmanns, 2018). The bioactive metabolites produced by the benthic dinoflagellate (Pavaux et al., 2020) may be detrimental or beneficial to the macroalgal host.

The bioactivity of the SEs combined to the natural settlement of *O.* cf. *ovata* suggests that the colonization preferences of *O.* cf. *ovata* are not driven by the sole bioactivity of the surface chemistry of macroalgae. Indeed, the highest abundance of *O.* cf. *ovata*'s cells were found on *D. dichotoma* that simultaneously presented the highest bioactivity at ecological concentrations (1 mg cm^{-2}). The toxicity of *D. dichotoma* surface chemistry is likely faded by other unknown factors that may include reduced grazing and interspecific competition as shown by the lower ratio dinoflagellates:maxillopods and dinoflagellates:diatoms observed at the surface of *D. dichotoma* compared to other macroalgae. Diterpenes of *Dictyota* spp. have been shown to have deterrent effects on a wide range of

herbivores (Hay and Steinberg, 1992; Pereira et al., 2000) and could also target grazers like copepods since they have been shown to be sensitive to various allelochemicals (Ianora et al., 2004). The lower bioactivity of *D. spiralis* SEs compared to those of *D. dichotoma* (tested at 2 mg cm^{-2}) could not explain the low abundance of *O.* cf. *ovata* on its surface, suggesting the existence of other inhibiting factors controlling the colonization of the dinoflagellate on this macroalga as for instance the large relative abundance of copepods compared to that found at the surface of *D. dichotoma*.

The outcome of this experiment considered neither a spatial nor temporal variability, and rather describes an interaction between macroalgae and *O.* cf. *ovata* at high temperature (∼24°C) and salinity (∼39) conditions commonly found in the NW Mediterranean coastal waters in summer (Vila et al., 2001). If *O.* cf. *ovata* mostly blooms in summer across the Mediterranean Sea (Ciminiello et al., 2006; Cohu et al., 2013), late blooms are also reported in several areas (Aligizaki and Nikolaidis, 2006; Accoroni et al., 2012). The macroalgae colonized by *O.* cf. *ovata* were shown to differ throughout the year (Aligizaki and Nikolaidis, 2006; Battocchi et al., 2010; Hosny and Labib, 2019) likely in link to the macroalgal seasonality that modifies both their distribution and chemotypes (Paix et al., 2019) as well as their related bioactivity (Salvador Soler et al., 2007). In addition, the growth of *O.* cf. *ovata* was shown to be salinity sensitive (Pistocchi et al., 2011) and is optimal at salinity 36. Salinity also determines the distribution of seaweeds species (Martins et al., 1999) by altering various physiological aspects, including the production of metabolites (Polo et al., 2015). Therefore, at lower salinities areas (e.g., Northern Adriatic) a modified macroalgal bioactivity may lead to a different colonization pattern by *O.* cf. *ovata* (Accoroni et al., 2016).

CONCLUSION

The present dataset confirms that some Phaeophyceae of the family Dictyotaceae like *T. atomaria*, *Dictyota* spp. or *P. pavonica* may be characterized by a lower abundance of *O.* cf. *ovata* cells. Whether the surface chemistry of the macroalgae have the potential to handicap the growth of *O.* cf. *ovata*, it is not enough to explain the settlement preference on *D. dichotoma* that was found to be the most bioactive species. Complex interlacing factors involving several members of the epiphytic community are likely to modulate the growth of the toxic benthic dinoflagellate *O.* cf. *ovata* on macroalgae.

DATA AVAILABILITY STATEMENT

The datasets presented in this study can be found in online repositories. The names of the repository/repositories and accession number(s) can be found below: NCBI Sequence Read Archive (SRA) (accession: PRJNA612893).

AUTHOR CONTRIBUTIONS

ET, BP, J-FB, and GC designed the experiments. ET and BP conducted the experiments and treated the data. All the authors participated in the analysis of the data, contributed to the manuscript and approved the submitted version.

FUNDING

This work benefited from the support of the project OCEAN-15 (ANR-15-CE35-0002-01) of the French National Research Agency (ANR) and from the project CMAPO (2017) of the French GdR Mediatec. This work was also funded by the French "Sud Provence-Alpes-Côte d'Azur (Sud PACA)" regional council (Ph.D. grant of BP). The open access publication was supported by the MSCA project CHEMICROS (H2020-MSCA-IF-841051).

ACKNOWLEDGMENTS

The authors are grateful to Anaïs Lebrun for her help with bioassays and to Dr. Stéphane Greff (Aix-Marseille University, IMBE) for his help during the acquisition of LC-MS profiles. LC-MS experiments were conducted on the regional platform MALLABAR funded by the Institute of Ecology and Environment (INEE) of the French National Centre for Scientific Research (CNRS) and the French Sud PACA regional council.

SUPPLEMENTARY MATERIAL

The Supplementary Material for this article can be found online at: https://www.frontiersin.org/articles/10.3389/fmars.2020.00683/full#supplementary-material

REFERENCES

Accoroni, S., Percopo, I., Cerino, F., Romagnoli, T., Pichierri, S., Perrone, C., et al. (2015). Allelopathic interactions between the HAB dinoflagellate *Ostreopsis* cf. ovata and macroalgae. *Harmful Algae* 49, 147–155. doi: 10.1016/j.hal.2015.08.007

Accoroni, S., Romagnoli, T., Pichierri, S., Colombo, F., and Totti, C. (2012). Morphometric analysis of *Ostreopsis* cf. ovata cells in relation to environmental conditions and bloom phases. *Harmful Algae* 19, 15–22. doi: 10.1016/j.hal.2012.05.003

Accoroni, S., Romagnoli, T., Pichierri, S., and Totti, C. (2016). Effects of the bloom of harmful benthic dinoflagellate *Ostreopsis* cf. ovata on the microphytobenthos community in the northern Adriatic Sea. *Harmful Algae* 55, 179–190. doi: 10.1016/j.hal.2016.03.003

Aligizaki, K., and Nikolaidis, G. (2006). The presence of the potentially toxic genera *Ostreopsis* and Coolia (Dinophyceae) in the North Aegean Sea. Greece. *Harmful Algae* 5, 717–730. doi: 10.1016/j.hal.2006.02.005

Battocchi, C., Totti, C., Vila, M., Masó, M., Capellacci, S., Accoroni, S., et al. (2010). Monitoring toxic microalgae *Ostreopsis* (dinoflagellate) species in coastal waters of the Mediterranean Sea using molecular PCR-based assay combined with light microscopy. *Mar. Pollut. Bull.* 60, 1074–1084. doi: 10.1016/j.marpolbul.2010.01.017

Benita, M., Dubinsky, Z., and Iluz, D. (2018). *Padina pavonica*: morphology and calcification functions and mechanism. *Am. J. Plant Sci.* 9, 1156–1168.

Bertalot, H. L., Witowski, A., and Metzeltin, D. (2000). "*Diatom flora* of marine coasts, Vol. 1 iconographia diatomologica: annotated diatom micrographs vol 7 Diversity - Taxonomy - Identification," in *Iconographia Diatomologica*, Ed. H. Lange (Grafenau: Koeltz).

Bianco, ÉM., Rogers, R., Teixeira, V. L., and Pereira, R. C. (2009). Antifoulant diterpenes produced by the brown seaweed *Canistrocarpus cervicornis*. *J. Appl. Phycol.* 21, 341–346. doi: 10.1007/s10811-008-9374-9

Blanfuné, A., Boudouresque, C. F., Grossel, H., and Thibaut, T. (2015). Distribution and abundance of *Ostreopsis* spp. and associated species (Dinophyceae) in the northwestern Mediterranean: the region and the macroalgal substrate matter. *Environ. Sci. Pollut. Res.* 22, 12332–12346. doi: 10.1007/s11356-015-4525-4

Boisnoir, A., Pavaux, A.-S., Schizas, N. V., Marro, S., Blasco, T., Lemée, R., et al. (2020). The use of stable isotopes to measure the ingestion rate of potentially toxic benthic dinoflagellates by harpacticoid copepods. *J. Exp. Mar. Biol. Ecol.* 524, 151285. doi: 10.1016/j.jembe.2019.151285

Carnicer, O., Guallar, C., Andree, K. B., Diogène, J., and Fernández-Tejedor, M. (2015). *Ostreopsis* cf. ovata dynamics in the NW Mediterranean Sea in relation to biotic and abiotic factors. *Non-Regul. Environ. Contam. Seaf. Contrib. ECsafeSEAFOOD EU Proj.* 143, 89–99. doi: 10.1016/j.envres.2015.08.023

Casabianca, S., Casabianca, A., Riobó, P., Franco, J. M., Vila, M., and Penna, A. (2013). Quantification of the Toxic Dinoflagellate *Ostreopsis* spp. by qPCR Assay in Marine Aerosol. *Environ. Sci. Technol.* 47, 3788–3795. doi: 10.1021/es305018s

Chen, L., Kieber, D. J., Amato, F., Vila, M., Viure, L., Alastuey, A., et al. (2020). *Dimethylsulfoniopropionate Concentrations in Mediterranean Coastal Water and Ambient Aerosols During Ostreopsis cf. ovata Blooms*. San Diego: Ocean Sciences-Meeting.

Ciminiello, P., Dell'Aversano, C., Fattorusso, E., Forino, M., Magno, G. S., Tartaglione, L., et al. (2006). The Genoa 2005 outbreak. Determination of putative palytoxin in Mediterranean *Ostreopsis ovata* by a new liquid chromatography tandem mass spectrometry method. *Anal. Chem.* 78, 6153–6159.

Cohu, S., Mangialajo, L., Thibaut, T., Blanfuné, A., Marro, S., and Lemée, R. (2013). Proliferation of the toxic dinoflagellate *Ostreopsis* cf. ovata in relation to depth, biotic substrate and environmental factors in the North West Mediterranean Sea. *Harmful Algae* 24, 32–44. doi: 10.1016/j.hal.2013.01.002

Cohu, S., Thibaut, T., Mangialajo, L., Labat, J. P., Passafiume, O., Blanfune, A., et al. (2011). Occurrence of the toxic dinoflagellate *Ostreopsis* cf. ovata in relation with environmental factors in Monaco (NW Mediterranean). *Mar. Pollut. Bull.* 62, 2681–2691. doi: 10.1016/j.marpolbul.2011.09.022

Debroas, D., Mone, A., and Ter Halle, A. (2017). Plastics in the North Atlantic garbage patch: a boat-microbe for hitchhikers and plastic degraders. *Sci. Total Environ.* 599–600, 1222–1232. doi: 10.1016/j.scitotenv.2017.05.059

Egan, S., Harder, T., Burke, C., Steinberg, P., Kjelleberg, S., and Thomas, T. (2013). The seaweed holobiont: understanding seaweed–bacteria interactions. *FEMS Microbiol. Rev.* 37, 462–476. doi: 10.1111/1574-6976.12011

Escudié, F., Auer, L., Bernard, M., Mariadassou, M., Cauquil, L., Vidal, K., et al. (2017). FROGS: find. Rapidly, OTUs with Galaxy Solution. *Bioinformatics* 34, 1287–1294. doi: 10.1093/bioinformatics/btx791

Faimali, M., Giussani, V., Piazza, V., Garaventa, F., Corrà, C., Asnaghi, V., et al. (2012). Toxic effects of harmful benthic dinoflagellate *Ostreopsis* ovata on invertebrate and vertebrate marine organisms. *Mar. Environ. Res.* 76, 97–107. doi: 10.1016/j.marenvres.2011.09.010

Furlan, M., Antonioli, M., Zingone, A., Sardo, A., Blason, C., Pallavicini, A., et al. (2013). Molecular identification of *Ostreopsis* cf. ovata in filter feeders and putative predators. *Harmful Algae* 21–22, 20–29. doi: 10.1016/j.hal.2012.11.004

García-Portela, M., Riobó, P., Franco, J. M., Bañuelos, R. M., and Rodríguez, F. (2016). Genetic and toxinological characterization of North Atlantic strains of the dinoflagellate *Ostreopsis* and allelopathic interactions with toxic and non-toxic species from the genera Prorocentrum, Coolia and Gambierdiscus. *Harmful Algae* 60, 57–69. doi: 10.1016/j.hal.2016.10.007

Gémin, M., Réveillon, D., Hervé, F., Pavaux, A., Tharaud, M., Séchet, V., et al. (2020). Toxin content of *Ostreopsis* cf. ovata depends on bloom phases, depth and macroalgal substrate in the NW Mediterranean Sea. *Harmful Algae* 92, 101727. doi: 10.1016/j.hal.2019.101727

Giussani, V., Costa, E., Pecorino, D., Berdalet, E., De Giampaulis, G., Gentile, M., et al. (2016). Effects of the harmful dinoflagellate *Ostreopsis* cf. ovata on different life cycle stages of the common moon jellyfish Aurelia sp. *Harmful Algae* 57, 49–58. doi: 10.1016/j.hal.2016.05.005

Goecke, F., Labes, A., Wiese, J., and Imhoff, J. (2010). Chemical interactions between marine macroalgae and bacteria. *Mar. Ecol. Prog. Ser.* 409, 267–299.

Gorbi, S., Avio, G. C., Benedetti, M., Totti, C., Accoroni, S., Pichierri, S., et al. (2013). Effects of harmful dinoflagellate *Ostreopsis* cf. ovata exposure on immunological, histological and oxidative responses of mussels Mytilus galloprovincialis. *Fish Shellfish Immunol.* 35, 941–950. doi: 10.1016/j.fsi.2013.07.003

Guidi, F., Pezzolesi, L., and Vanucci, S. (2018). Microbial dynamics during harmful dinoflagellate *Ostreopsis* cf. ovata growth: bacterial succession and viral abundance pattern. *MicrobiologyOpen* 7:e00584. doi: 10.1002/mbo3.584

Guidi-Guilvard, L. D., Gasparini, S., and Lemée, R. (2012). The Negative Impact of *Ostreopsis* cf. Ovata on Phytal Meiofauna from the Coastal NW Mediterranean. *Cryptogam. Algol.* 33, 121–128. doi: 10.7872/crya.v33.iss2.2011.121

Guillard, R. R. L., and Ryther, J. H. (1962). Studies of marine planktonic diatoms; I. Cyclotella nana Hustedt, and Detonula Confervacea (Cleve) Gran. *Can. J. Microbiol.* 8, 229–239. doi: 10.1139/m62-029

Hay, M., and Steinberg, P. (1992). "The chemical ecology of plant-herbivore interactions in marine versus terrestrial communities," in *Herbivores: Their Interaction with Secondary Plant Metabolites., Evolutionary and Ecological Processes*, eds G. A. Rosenthal, and M. R. Berenbaum (New York, NY: Elsevier Science), 371–413.

Hellio, C., Berge, J. P., Beaupoil, C., Le Gal, Y., and Bourgougnon, N. (2002). Screening of Marine Algal Extracts for Anti-settlement Activities against Microalgae and Macroalgae. *Biofouling* 18, 205–215. doi: 10.1080/08927010290010137

Hollants, J., Leliaert, F., De Clerck, O., and Willems, A. (2013). What we can learn from sushi: a review on seaweed–bacterial associations. *FEMS Microbiol. Ecol.* 83, 1–16. doi: 10.1111/j.1574-6941.2012.01446.x

Horiguchi, E. (ed.) (2014). *Marine Benthic Dinoflagellates - Unveiling Their Worldwide Biodiversity*. Stuttgart: Schweizerbart Science Publishers.

Hosny, S., and Labib, W. (2019). Ecology of the Epiphytic Potentially Harmful Dinoflagellate *Ostreopsis* cf. ovata (Fukuyo) from Coastal Waters off Alexandria Egypt. *J. Ocean Mar. Res.* 7:2.

Ianora, A., Miralto, A., Poulet, S. A., Carotenuto, Y., Buttino, I., Romano, G., et al. (2004). Aldehyde suppression of copepod recruitment in blooms of a ubiquitous planktonic diatom. *Nature* 429, 403–407. doi: 10.1038/nature02526

Jauzein, C., Açaf, L., Accoroni, S., Asnaghi, V., Fricke, A., Hachani, M. A., et al. (2018). Optimization of sampling, cell collection and counting for the monitoring of benthic harmful algal blooms: application to *Ostreopsis* spp. blooms in the Mediterranean Sea. *Ecol. Indic.* 91, 116–127. doi: 10.1016/j.ecolind.2018.03.089

Kim, J. Y., Alamsjah, M. A., Hamada, A., Fujita, Y., and Ishibashi, F. (2006). Algicidal Diterpenes from the Brown Alga *Dictyota dichotoma*. *Biosci. Biotechnol. Biochem.* 70, 2571–2574. doi: 10.1271/bbb.60281

Mahé, F., Rognes, T., Quince, C., de Vargas, C., and Dunthorn, M. (2014). Swarm: robust and fast clustering method for amplicon-based studies. *PeerJ* 2:e593.

Mangialajo, L., Ganzin, N., Accoroni, S., Asnaghi, V., Blanfune, A., Cabrini, M., et al. (2011). Trends in *Ostreopsis* proliferation along the Northern Mediterranean coasts. Toxicon Off. *J. Int. Soc. Toxinology* 57, 408–420. doi: 10.1016/j.toxicon.2010.11.019

Marro, S., Pavaux, A.-S., Drouet, K., and Lemée, R. (2019). "Diversity of benthic microphytoplankton associated to *Ostreopsis* cf. ovata bloom in the NW Mediterranean Sea," in *Poster at French National Conference on HAB*, (Brest: PHYCOTOX Group), 1.

Martins, I., Oliveira, J. M., Flindt, M. R., and Marques, J. C. (1999). The effect of salinity on the growth rate of the macroalgae Enteromorpha intestinalis (Chlorophyta) in the Mondego estuary (west Portugal). *Acta Oecol.* 20, 259–265. doi: 10.1016/S1146-609X(99)00140-X

McMurdie, P. J., and Holmes, S. (2013). phyloseq: an R Package for Reproducible Interactive Analysis and Graphics of Microbiome Census Data. *PLoS One* 8:e61217. doi: 10.1371/journal.pone.0061217

Meroni, L., Chiantore, M., Petrillo, M., and Asnaghi, V. (2018). Habitat effects on *Ostreopsis* cf. ovata bloom dynamics. *Harmful Algae* 80, 64–71. doi: 10.1016/j.hal.2018.09.006

Monti, M., and Cecchin, E. (2012). Comparative growth of three strains of *Ostreopsis ovata* at different light intensities with focus on inter-specific

allelopathic interactions. *Cryptogam. Algol.* 33, 113–119. doi: 10.7872/crya.v33.iss2.2011.113

Nagayama, K., Shibata, T., Fujimoto, K., Honjo, T., and Nakamura, T. (2003). Algicidal effect of phlorotannins from the brown alga Ecklonia kurome on red tide microalgae. *Aquaculture* 218, 601–611. doi: 10.1016/S0044-8486(02)00255-7

Oksanen, J., Blanchet, F. G., Kindt, R., Legendre, P., Minchin, P. R., O'hara, R., et al. (2013). Package 'vegan.'. *Commun. Ecol. Package Version* 2, 1–295.

Othmani, A., Briand, J.-F., Ayé, M., Molmeret, M., and Culioli, G. (2016a). Surface metabolites of the brown alga Taonia atomaria have the ability to regulate epibiosis. *Biofouling* 32, 801–813. doi: 10.1080/08927014.2016.1198954

Othmani, A., Bunet, R., Bonnefont, J.-L., Briand, J.-F., and Culioli, G. (2016b). Settlement inhibition of marine biofilm bacteria and barnacle larvae by compounds isolated from the Mediterranean brown alga *Taonia atomaria*. *J. Appl. Phycol.* 28, 1975–1986. doi: 10.1007/s10811-015-0668-4

Paix, B., Carriot, N., Barry-Martinet, R., Greff, S., Misson, B., Briand, J.-F., et al. (2020). A Multi-Omics analysis suggests links between the differentiated surface metabolome and epiphytic microbiota along the thallus of a mediterranean seaweed holobiont. *Front. Microbiol.* 11:494. doi: 10.3389/fmicb.2020.00494

Paix, B., Othmani, A., Debroas, D., Culioli, G., and Briand, J.-F. (2019). Temporal covariation of epibacterial community and surface metabolome in the Mediterranean seaweed holobiont *Taonia atomaria*. *Environ. Microbiol.* 21, 3346–3363. doi: 10.1111/1462-2920.14617

Pavaux, A.-S., Rostan, J., Guidi-Guilvard, L., Marro, S., Ternon, E., Thomas, O. P., et al. (2019). Effects of the toxic dinoflagellate *Ostreopsis* cf. ovata on survival, feeding and reproduction of a phytal harpacticoid copepod. *J. Exp. Mar. Biol. Ecol.* 516, 103–113. doi: 10.1016/j.jembe.2019.05.004

Pavaux, A.-S., Ternon, E., Dufour, L., Marro, S., Gémin, M.-P., Thomas, O. P., et al. (2020). Efficient, fast and inexpensive bioassay to monitor benthic microalgae toxicity: application to *Ostreopsis* species. *Aquat. Toxicol.* 223:105485. doi: 10.1016/j.aquatox.2020.105485

Pereira, R. C., Cavalcanti, D. N., and Teixeira, V. L. (2000). Effects of secondary metabolites from the tropical Brazilian brown alga Dictyota menstrualis on the amphipod Parhyale hawaiensis. *Mar. Ecol. Prog. Ser.* 205, 95–100.

Pezzolesi, L., Guerrini, F., Ciminiello, P., Dell'Aversano, C., Dello Iacovo, E., Fattorusso, E., et al. (2012). Influence of temperature and salinity on *Ostreopsis* cf. ovata growth and evaluation of toxin content through HR LC-MS and biological assays. *Water Res.* 46, 82–92. doi: 10.1016/j.watres.2011.10.029

Pistocchi, R., Pezzolesi, L., Guerrini, F., Vanucci, S., Dell'aversano, C., and Fattorusso, E. (2011). A review on the effects of environmental conditions on growth and toxin production of *Ostreopsis* ovata. *Toxicon Off. J. Int. Soc. Toxinol.* 57, 421–428. doi: 10.1016/j.toxicon.2010.09.013

Polo, L. K., Felix, M. R. L., Kreusch, M., Pereira, D. T., Costa, G. B., Simioni, C., et al. (2015). Metabolic profile of the brown macroalga Sargassum cymosum (Phaeophyceae, Fucales) under laboratory UV radiation and salinity conditions. *J. Appl. Phycol.* 27, 887–899. doi: 10.1007/s10811-014-0381-8

Poulson-Ellestad, K. L., Jones, A., Roy, J., Viant, M. R., Fernandez, F. M., Kubanek, J., et al. (2014). Metabolomics and proteomics reveal impacts of chemically mediated competition on marine phytoplankton. *PNAS* 111, 9009–9014. doi: 10.1073/pnas.1413432111

Prato, E., Biandolino, F., Bisci, A. P., and Caroppo, C. (2011). Preliminary assessment of *Ostreopsis* cfr. ovata acute toxicity by using a battery bioassay. *Chem. Ecol.* 27, 117–125. doi: 10.1080/02757540.2011.625930

Puglisi, M. P., Sneed, J. M., Sharp, K. H., Ritson-Williams, R., and Paul, V. J. (2014). Marine chemical ecology in benthic environments. *Nat. Prod. Rep.* 31, 1510–1553. doi: 10.1039/C4NP00017J

Rognes, T., Flouri, T., Nichols, B., Quince, C., and Mahé, F. (2016). VSEARCH: a versatile open source tool for metagenomics. *PeerJ* 4:e2584.

Saha, M., Rempt, M., Gebser, B., Grueneberg, J., Pohnert, G., and Weinberger, F. (2012). Dimethylsulphopropionate (DMSP) and proline from the surface of the brown alga Fucus vesiculosus inhibit bacterial attachment. *Biofouling* 28, 593–604. doi: 10.1080/08927014.2012.698615

Saha, M., Rempt, M., Grosser, K., Pohnert, G., and Weinberger, F. (2011). Surface-associated fucoxanthin mediates settlement of bacterial epiphytes on the rockweed *Fucus vesiculosus*. *Biofouling* 27, 423–433. doi: 10.1080/08927014.2011.580841

Saha, M., and Weinberger, F. (2019). Microbial "gardening" by a seaweed holobiont: Surface metabolites attract protective and deter pathogenic epibacterial settlement. *J. Ecol.* 107, 2255–2265. doi: 10.1111/1365-2745.13193

Salvador Soler, N., Gomez Garreta, M. A., Lavelli, L., and Ribera Siguan, M.-A. (2007). Antimicrobial Activity of Iberian macroalgae. *Sci. Mar.* 71, 101–113.

Schmitt, T. M., Lindquist, N., and Hay, M. E. (1998). Seaweed secondary metabolites as antifoulants: effects of Dictyota spp. diterpenes on survivorship, settlement, and development of marine invertebrate larvae. *Chemoecology* 8, 125–131. doi: 10.1007/s000490050017

Selander, E., Kubanek, J., Hamberg, M., Andersson, M. X., Cervin, G., and Pavia, H. (2015). Predator lipids induce paralytic shellfish toxins in bloom-forming algae. *Proc. Natl. Acad. Sci. U.S.A.* 112, 6395–6400. doi: 10.1073/pnas.1420154112

Simonini, R., Orlandi, M., and Abbate, M. (2011). Is the toxic dinoflagellate *Ostreopsis* cf. ovata harmful to Mediterranean benthic invertebrates? Evidences from ecotoxicological tests with the polychaete *Dinophilus gyrociliatus*. *Mar. Environ. Res.* 72, 230–233. doi: 10.1016/j.marenvres.2011.08.009

Smith, C. A., Want, E. J., O'Maille, G., Abagyan, R., and Siuzdak, G. (2006). XCMS: Processing Mass Spectrometry Data for Metabolite Profiling Using Nonlinear Peak Alignment. Matching, and Identification. *Anal. Chem.* 78, 779–787. doi: 10.1021/ac051437y

Tait, K., Joint, I., Daykin, M., Milton, D. L., Williams, P., and Cámara, M. (2005). Disruption of quorum sensing in seawater abolishes attraction of zoospores of the green alga Ulva to bacterial biofilms. *Environ. Microbiol.* 7, 229–240. doi: 10.1111/j.1462-2920.2004.00706.x

Tang, Y. Z., and Gobler, C. J. (2011). The green macroalga, Ulva lactuca, inhibits the growth of seven common harmful algal bloom species via allelopathy. *Harmful Algae* 10, 480–488. doi: 10.1016/j.hal.2011.03.003

Ternon, E., Pavaux, A.-S., Marro, S., Thomas, O. P., and Lemée, R. (2018). Allelopathic interactions between the benthic toxic dinoflagellate *Ostreopsis* cf. ovata and a co-occurring diatom. *Harmful Algae* 75, 35–44. doi: 10.1016/j.hal.2018.04.003

Tillmann, U., and Hansen, P. (2009). Allelopathic effects of *Alexandrium tamarense* on other algae: evidence from mixed growth experiments. *Aquat. Microb. Ecol.* 57, 101–112.

Totti, C., Accoroni, S., Cerino, F., Cucchiari, E., and Romagnoli, T. (2010). *Ostreopsis* ovata bloom along the Conero Riviera (northern Adriatic Sea): relationships with environmental conditions and substrata. *Harmful Algae* 9, 233–239. doi: 10.1016/j.hal.2009.10.006

Tsushima, M., Maoka, T., and Matsuno, T. (2001). Structures of Carotenoids with 5,6-Dihydro-β-End Groups from the Spindle Shell Fusinus perplexus. *J. Nat. Prod.* 64, 1139–1142. doi: 10.1021/np010060y

Vanucci, S., Guidi, F., Pistocchi, R., and Long, R. A. (2016). Phylogenetic structure of bacterial assemblages co-occurring with *Ostreopsis* cf. ovata bloom. *Harmful Algae* 55, 259–271. doi: 10.1016/j.hal.2016.04.003

Viano, Y., Bonhomme, D., Camps, M., Briand, J.-F., Ortalo-Magné, A., Blache, Y., et al. (2009). Diterpenoids from the Mediterranean Brown Alga Dictyota sp. Evaluated as Antifouling Substances against a Marine Bacterial Biofilm. *J. Nat. Prod.* 72, 1299–1304. doi: 10.1021/np900102f

Vila, M., Garcés, E., and Maso, M. (2001). Potentially toxic epiphytic dinoflagellate assemblages on macroalgae in the NW Mediterranean. *Aquat. Microb. Ecol.* 26, 51–60.

Wheeler, G. L., Tait, K., Taylor, A., Brownlee, C., and Joint, I. (2006). Acyl-homoserine lactones modulate the settlement rate of zoospores of the marine alga Ulva intestinalis via a novel chemokinetic mechanism. *Plant Cell Environ.* 29, 608–618. doi: 10.1111/j.1365-3040.2005.01440.x

Wichard, T., and Beemelmanns, C. (2018). Role of Chemical Mediators in Aquatic Interactions across the Prokaryote–Eukaryote Boundary. *J. Chem. Ecol.* 44, 1008–1021. doi: 10.1007/s10886-018-1004-7

Conflict of Interest: The authors declare that the research was conducted in the absence of any commercial or financial relationships that could be construed as a potential conflict of interest.